Title

Further investigations of a radiation detector based on ionization-induced modulation of optical polarization.

Journal

Physics in Medicine & Biology, 66(5)

Authors

Wang, Yuli
Tao, Li
Abbaszadeh, Shiva
et al.

Publication Date

2021-02-20

DOI

10.1088/1361-6560/abe027

Peer reviewed

HHS Public Access

Author manuscript

Phys Med Biol. Author manuscript; available in PMC 2021 April 20.

Published in final edited form as:

Phys Med Biol. ; 66(5): 055013. doi:10.1088/1361-6560/abe027.

Further investigations of a radiation detector based on ionization-induced modulation of optical polarization

Yuli Wang[1], **Li Tao**[2], **Shiva Abbaszadeh**[1], **Craig Levin**[2]

[1]Department of Electrical and Computer Engineering, University of California, Santa Cruz, Santa Cruz, CA, 95064, United States of America

[2]Molecular Imaging Instrumentation Laboratory, Stanford University, Stanford, CA 94305, United States of America

Abstract

Optical property modulation induced by ionizing radiation is a promising approach for ultra-fast, lower time jitter detection of photon arrival time. If successful, this method can be utilized in time-of-flight positron emission tomography to achieve a coincidence time resolution approaching 10 ps. In this work, the optical property modulation based method is further developed with focus on a detection setup based on two crossed polarizers. Previous work demonstrated that such an optical setup could be utilized in radiation detection, though its detection sensitivity needed improvement. This work investigates the angle between polarizers and electric field distribution within the detection crystal to understand and improve the detection sensitivity of an optical polarization modulation based method. For this work, cadmium telluride (CdTe) was studied as the detector crystal. The 'magic' angle (i.e. optimal working angle) of the two crossed polarizers based optical setup with CdTe were explored theoretically and experimentally. The experimental results show that the detection sensitivity could be improved by around 10% by determining the appropriate 'magic' angle. We then studied the dependence of detection sensitivity on electric field distribution as well as on the bias voltage across the detector crystal using CdTe crystals. The experimental results show that a smaller electrode on the detector crystal, or a more concentrated electric field distribution could improve detection sensitivity. For CdTe, a detector crystal sample with 2.5 mm × 2.5 mm square electrode has twice the detection sensitivity of a detector crystal with 5 mm × 5 mm square electrode. Increasing the bias voltage before saturation for CdTe could further enhance the modulation strength and thus, the sensitivity. Our investigations demonstrated that by determining the proper working angle of polarizers and bias electrical distribution to the detector, we could improve the sensitivity of the proposed optical setup.

Keywords

positron emission tomography; optical property modulation; cadmium telluride (CdTe); time-of-flight (TOF)

cslevin@stanford.edu.

1. Introduction

Positron emission tomography (PET) is a non-invasive medical imaging technology that visualizes and quantifies the molecular bases of diseases such as cancer, heart disease and neurological disorders. A sub-10 picosecond (ps) coincidence time resolution (CTR) is a new target for next generation time-of-flight-PET (Lecoq 2012) and an improved CTR could benefit the image reconstruction process, especially leading to significant gains in image signal-to-noise ratio (SNR). The SNR boost could decrease patient's necessary injected radiation dose (Surti *et al* 2011), or be utilized to shorten scan time (Fakhir *et al* 2011), reduce sensitivity to errors in data correction techniques (Turkington and Wilson 2009) and improve precision of lesion uptake measurement (Daube-Witherspoon *et al* 2014).

However, the CTR is mainly limited by the scintillation process which has an intrinsic limit around 100 ps (Lecoq 2017) full-width-at-half-maximum. Many researchers have focused on improving scintillation crystal properties and exploring alternate detection mechanisms with the potential for better temporal resolution. For example, multiple studies are based on the scintillator crystal dimension. Small crystals (e.g. 3 mm length) have been studied for fast time research (Gundacker *et al* 2014, Nemallapudi *et al* 2015, Cates and Levin 2016), as well as side readout of long crystals (Cates and Levin 2018), since both approaches reduce the temporal variance in the scintillation light transition and collection. Doping element concentration of the scintillator crystals is another parameter for achieving fast-timing detection. Studies on light yield, energy resolution and light transmission were performed on various cerium doped LYSO/LGSO scintillators which were used as the phoswich detector (Pepin *et al* 2010, Loignon-Houle *et al* 2014, Bergeron *et al* 2015). Cerenkov radiation (Dothager *et al* 2010, Cates and Levin 2019) as well as radiation detection using nanostructure in crystals have also been explored as fast-time methods (Turtos *et al* 2016).

To achieve sub-10 ps time resolution, efforts have been made in using scintillator crystals as detector materials (Cates and Levin 2016, 2018, Gundacker *et al* 2016). As another way to achieve ionization radiation detection that shows promise to significantly improve the CTR, a new detection method was proposed that utilizes optical property modulation (Tao *et al* 2016, 2017, 2020). Previously, an optical pump-probe concept was used to implement a setup with two crossed polarizers for the detection of ionizing radiation (Wang *et al* 2019a). The optical setup utilized the Pockels effect and pump-probe measurement as the detection mechanism. The performance of the proposed experimental setup with Lithium Niobate (LiNbO3) and cadmium telluride (CdTe) as detector crystals was evaluated, and the desired properties of an ideal detector crystal were discussed. However, there still exist significant technical challenges to using optical property modulation based detection, particularly due to the need to dramatically improve the detection sensitivity of the setup to achieve single 511 KeV photon detection.

This paper will first briefly introduce our experimental setup for two crossed polarizers and discuss the theory of the detection mechanism. The magic angle (Howe-Siang *et al* 2005) of our optical property modulation based setup was investigated theoretically and experimentally. The detection sensitivity can be improved by setting the polarizers' working angle at its magic angle. Moreover, the paper investigates the dependence of detection

sensitivity on electric field distribution in order to study other influencing factors on the setup detection sensitivity.

2. Materials and methods

2.1. Material selection for ionizing radiation detector

Cubic CdTe detector crystals with 5 mm on a side dimension (Gooch & Housego, Moorpark, CA, USA) were used in this study. All crystal surfaces were polished with electrodes deposited on two opposite surfaces of each crystal for adding bias voltage. Crystal characteristics including dimensions, refractive index, density, effective Z number, band gap energy, Pockels effect coefficient and resistivity are summarized in table 1.

CdTe was the detector used in our previous work (Wang *et al* 2019a, 2019b). This material has been widely used in photonics devices as ultra-fast switches due to its high density and high effective Z number, which could improve the interaction probability between the detector crystal and the ionizing photon.

2.2. Experimental setup

A new detection concept, utilizing optical pump-probe measurement, has been demonstrated for ionizing radiation detection (Tao *et al* 2016). We previously employed this concept with an optical setup based on two crossed polarizers to detect ionizing radiation (Wang *et al* 2019a). The schematic arrangement of that optical setup is shown in figure 1. A tunable laser beam is first collimated, then the laser light transmits through the first polarizer. The linear polarized laser light from the first polarizer illuminates the front of the detector crystal and exits the crystal from the back side. The exiting light goes into the second crossed polarizer, followed by a focusing lens and a high sensitivity photodiode. Transmitted light intensity is the signal being monitored during the experiment. When the ionizing radiation source is not present, nominally the cross-polarizers cancel the transmitted signal. When ionization occurs within the detector crystal, this transiently perturbs the linear polarization of the light entering the crystal, allowing some non-polarized light to transmit through the second polarizer and generate a signal in the photodetector. The detector crystal is biased and the whole setup is placed in a light-tight box during the experiment.

In this paper, we are going to use the two-crossed-polarizer setup to explore approaches to improve the detection sensitivity for the optical property modulation-based method.

2.3. Detection theory

In this work, the Pockels effect is used to measure the optical property modulation induced by radiation, which could modify the refractive index of each detector crystal due to the interaction between the crystal and the ionizing radiation photons. Detector crystals are regarded as Pockels cells and the induced refractive index of each Pockels cell (Ironside 2017) can be expressed by equation (1):

$$n(E) \approx n_0 - \frac{1}{2}\gamma n_0^3 E, \tag{1}$$

where $n(E)$ is the refractive index of a detector crystal with an applied electric field E, E is the applied bias voltage, including the external voltage from a high voltage power supply and the internal bias voltage induced by the interaction between the detector crystal and ionizing radiation photons, γ is the coefficient of the Pockels effect, and n_0 is the refractive index of the detector crystal without bias voltage.

The dependence of transmitted light intensity on applied bias voltage is expressed as equation (2):

$$I = I_0 \cos^2\left(\frac{\pi n(E)\gamma d E}{\lambda}\right), \tag{2}$$

where I is the intensity of transmitted light through two crossed polarizers, I_0 is the maximum intensity of transmitted light through two crossed polarizers, d is the path length of light through the crystal, which approximately equals the thickness of the detector crystal, λ is the wavelength of the probe laser, and $n(E)$, γ, E have the same meanings in equation (1).

Charge carriers are generated when the ionizing radiation photon interacts with the detector crystal. After generation, charge carriers immediately drift toward two opposite electrodes under the external applied bias voltage, producing an internal electrical field opposite to the external electrical field. In other words, local charge carrier separation will result in a disturbance in the distribution of the electric field within the crystal. According to equation (1), after an ionizing radiation interaction, the refractive index of the detector crystal would be modulated as a result. According to equation (2), the change of refractive index of the crystal would modify the polarization state of transmitted light through the crystal and then change the intensity of transmitted light through the second polarizer, which would ultimately modify the output of the photodiode. Therefore, monitoring the output of photodetector could achieve the goal to monitor the interaction of ionizing radiation.

2.4. Investigation on the magic angle of the two cross-polarizers setup

The polarization-selective technique (Terance 1969) is widely used in many time-resolved optical experiments, since the optical elements in the experiment setup would inevitably affect the polarization of light. Therefore, experiments have been designed to explore the influence of experimental configuration and optical elements of a setup. The optimal working position of the linear polarizers in this experiment is called the magic angle (Tkachenko 2006). The theory of polarization sensitive experiments has been well developed (Tokmakoff 1996). However, in theoretical studies, many practical factors were not taken into consideration, especially for optical setups with two crossed polarizers. In this paper, the magic angle of our setup was explored from both theoretical and experimental aspects.

2.4.1. Theoretical analysis—*The Weber–Fechner law* (Hecht 1924) describes the relationship between the magnitude of a physical stimulus and the intensity or strength of the corresponding detector response. *The Weber–Fechner law* can be expressed as equation (3):

$$S = K \ln R, \tag{3}$$

where S is the intensity or strength of the detector response, K is a constant factor that is a property of the detector, which takes into account the influence of the risetime, the bandwidth, the responsivity and the noise equivalent power of the detector, and R is the strength of stimulus. In this paper, stimulus is the transmitted intensity change of the probe laser beam after it passes through both polarizers. By taking the derivatives of both sides in equation (3), we arrive at equation (4):

$$dS = K\frac{dR}{R}, \tag{4}$$

where dS is the differential change of response intensity or strength, and dR is the differential increase or decrease in the stimulus. K and R have the same definition as in equation (3).

To analyze the magic angle in a two-crossed-polarizers setup, we also take the light transmission law—*Malus' law* (Collett 2005) into consideration, which states the relationship between the intensity of a plane-polarized light beam passing through polarizers and the working angle of polarizers. The light passing through two crossed polarizers is given by equation (5):

$$I = I_0 \cos^2\theta, \tag{5}$$

where I_0 is the initial light intensity, I is the intensity of transmitted light and θ is the angle between the laser beam's initial polarization direction and the axis of the polarizer. In this paper, θ is the angle between the first polarizer and the second polarizer. I_0 is a constant value. A close inspection reveals that equation (2) described in section 2.3 is exactly the same as *Malus' law* shown in equation (5). The dependence of light intensity I on working angle θ is shown in figure 2(a).

If we take the derivative of I with respect to the working angle θ, we have equation (6):

$$dI/d\theta = -I_0 \sin 2\theta, \tag{6}$$

where dI is the differential intensity change of transmitted light, I_0 and θ have the same meaning as in equation (5). The dependence of $dI/d\theta$ (light intensity differential) on the working angle θ is shown in figure 2(b).

In our experiment, according to *Weber–Fechner law*, the intensity or strength of stimulus R is the light intensity I; the differential increase in stimulus dR is the differential intensity change of transmitted light dI. Therefore, we substitute equation (6) into equation (4) to arrive at equation (7), and further arrive at equation (8)

$$dS = K\frac{dI}{I} = k\frac{-I_0 \sin 2\theta d\theta}{I_0 \cos^2\theta} = -2K \tan\theta d\theta \tag{7}$$

$$dS/d\theta = -2K\tan\theta\,. \tag{8}$$

All symbols have the same meanings as in equations (4)–(6). The dependence of $dS/d\theta$ (detector response differential) on the working angle θ is shown in figure 2(c).

Theoretical analysis of the magic angle of an optical setup based on two crossed polarizers can be summarized in table 2, including light intensity (LI) (I), light intensity differential ($dI/d\theta$) and detector response differential ($dS/d\theta$). LI represents the strength of light passing through the second polarizer. An observed LI differential represents the change ratio of light intensity. In other words, it represents the rate at which the light intensity changes as working angle changes. The detector response differential is the factor we may employ to directly evaluate the detection ability of the crossed-polarizer method and to determine its detection errors. The larger the detector response differential is, the more sensitive the detector. For a clear theoretical analysis, we quantitatively define the detection error as (Light Intensity differential)/(Detector response differential) to evaluate the detection sensitivity of each working angle, which is shown in equation (9). LI, LI differential, Detector response differential and Detection error are calculated theoretically at four different angles which are shown in table 2.

$$\text{Detection error } = \frac{dI/d\theta}{dS/d\theta} = \frac{-I_0\sin 2\theta}{-2K\tan\theta} = \frac{I_0}{K}\cos\theta\,. \tag{9}$$

Based on the theoretical calculations on table 2, our analysis of different working angles of two-cross-polarizers based setup can be summarized as follows:

- When $\theta = 0°$, LI differential and detector response differential are both zero, and LI passing through the second polarizer is at the largest value point. Using this point to detect, the final detected signal has the largest detection error ($2I_0/K$).
- When $\theta = 45°$, LI differential has the largest value when compared with other working angles, but detector response differential is not large enough to satisfy the accurate detection requirements of our setup (normally, the value of detector response differential should be larger than $10K$ for accurate detection (Hecht 1924)), and thus there is still relatively large detection error ($0.5I_0/K$) when setting this point as the polarizers' working point.
- When $\theta = 90°$, Detector response differential reaches infinity which means that the detector has the highest detection capability. Using this point to detect the modulated signal in our setup, the smallest detection errors 0 are expected theoretically. However, due to a minimum detection sensitivity limit existing in every detector, it requires the value of LI to be bigger than the detection sensitivity limit. If the value of LI and LI differential are almost 0, it means that the minimum detection visual threshold of the photodiode could not be achieved and results in detection error. Therefore, there still exists relatively large detection error at 90°, compared with the optimal working angle.

- When $86.5° \leqslant \theta \leqslant 89.5°$, light intensity is stronger or equal to the minimum detection sensitivity limit of the photodiode used in our experiment. We think the optimal working angle of our setup is in the region from 86.5° to 89.5°. This is further discussed in section 3.

2.4.2. Experimental measurement—Based on the theoretical analysis, we can estimate that the magic angle in our setup is approximately in the region from 88.0° to 91.0°. The following experiments were designed to determine the precise value of the magic angle. A $5 \times 5 \times 5$ mm^3 CdTe were chosen as the detector crystals, both of which were under a bias voltage of 1000 V during the experiments. For CdTe crystal, CdTe was then exposed to a 405 nm pump laser as the working angle between polarizers was adjusted around the theoretical range, in 0.05° deg/steps. A 405 nm (which is above the bandgap energy of the CdTe crystal) laser diode was used in our experiment as the ionizing radiation source to irradiate the crystal and to generate ionizing radiation charges. Due to its controllable emission timing and power, the laser diode could be a good shutter to start/end our observations of the modulated signal during the experiment. The laser diode was driven by a 100 Hz, 6V bias voltage with a pulse duration of 1 ms during the experiments. The frequency of the driving voltage was set 100 Hz in order to allow the induced charge carriers to recombine completely and allow complete recovery of the signal back to the level in the dark (original status). We used an oscilloscope to record the modulated signal by the laser diode. Afterwards, the same experimental arrangement and procedure were repeated for another two times for CdTe.

All results from the experiments are shown in section 3. The theoretical analysis and experimental process for finding the crystal's magic angle are not only limited to CdTe crystals but could be applied to all crystals. CdTe crystals are chosen as the example for magic angle investigating in this paper.

2.5. Investigating the dependence of detection sensitivity on electric field distribution

The modulation mechanism used in this work is Pockels effect, as shown in equation (1). The relationship between the intensity of light passing through two crossed polarizers and the applied electric field can be expressed as equation (2). These two equations are directly influenced by the applied electric field (including both the internal electric and external electric fields). Therefore, we investigated the optimal electric field distribution for our setup from simulations and experiments aiming to study the dependence of detection sensitivity on electric field distribution.

2.5.1. Selection of crystal electrodes and ionizing radiation sources—Polished $5 \times 5 \times 5$ mm^3 CdTe crystals, with two opposite surfaces deposited with Au electrodes, were used as Pockels cells. Three different electrode patterns for CdTe crystal were investigated, including a 5×5 mm^2 square planar electrode (5 × 5 electrode CdTe), a 4×4 mm^2 square planar electrode (4 × 4 electrode CdTe), and a 2.5×2.5 mm^2 square planar electrode (2.5 × 2.5 electrode CdTe).

2.5.2. Simulation studies based on Matlab—To find the optimal electric field distribution for our setup, we first simulated the electric field distribution by Partial Differential Equation tool box using Matlab. During the simulation, we build a 5 × 5 × 5 mm^3 cubic volume as our CdTe detector crystal. Given bias voltages (10V for anode electrode and −10V for cathode electrode chosen as the example in this paper) were added to two opposite surfaces of each detector crystal by different electrodes. 5 × 5 mm^2, 4 × 4 mm^2 and 2.5 × 2.5 mm^2 square electrodes are studied in our simulation.

Output results are formatted as 3D electric field distribution, 2D electric field distribution and direction of scaled E at grid point, respectively. For direction of scaled E at grid point, each value of E was scaled to itself in order to have a unit arrow length and a clear comparison. All results correspond to specific locations over the whole crystal and simulation results are shown in section 3.

2.5.3. Experiment to measure Pockels cell response—Pockels cell characteristics curves for CdTe crystals were obtained by recording the output signal magnitude of the photodiode with the crystal bias voltage changing in 80 V increments, ranging from 0 to 2000 V. The measurements verified the behavior of Pockels cells and also identified which electrode pattern leads to the strongest response to the Pockels effect. 5 × 5 electrode CdTe was first tested. We then repeated the same experiment for 4 × 4 electrode CdTe and 2.5 × 2.5 electrode CdTe. Results are shown in section 3.

2.5.4. Experiment with Ge-68 as ionizing radiation source—A Ge-68 isotope source was used as an ionizing radiation source to test the dependence of detection sensitivity on electric field distribution.

A 100 μCi of Ge-68 was repeatedly placed 15 mm away from the detector crystal and then removed. The change of optical signal between source present and source removed was recorded. The selected data point for each measurement was the stable signal level observed at five minutes after the source was placed or removed. Each data point (the stable signal level) was recorded as a histogram of the signal magnitudes for 30 s. Bias voltage added to the crystal was adjusted in 100 V increments from 0 to 2000 V. The experimental procedure is the same as the measurement of Pockels cell response for 5 × 5 electrode CdTe, 4 × 4 electrode CdTe and 2.5 × 2.5 electrode CdTe. The results are shown in section 3.

3. Results

3.1. Experimental results of magic angle

An example of the optical modulation signal induced by the laser diode as ionizing radiation source for CdTe is shown in figure 3. The maximum value of the optical signal magnitude is marked as ‘MAX’, while the minimum value of the optical signal magnitude is marked as ‘MIN’. The optical modulation strength is defined as ‘(MAX − MIN)/(MAX + MIN)’ to represent the detection sensitivity of our experiment setup. This definition is borrowed from previous work (Li *et al* 2018). Bigger ‘(MAX − MIN)/(MAX + MIN)’ value indicates better detection sensitivity. By comparing these ‘(MAX − MIN)/(MAX + MIN)’ values recorded under different cross-polarizers’ working angles, we can find the optimal working angle

(magic angle) of our optical setup. Figure 4(a) shows the optical modulation strength for CdTe detector crystal with different working angles. Average value and 95% confidence interval analysis of three experiments are shown in figure 4(b). In order to exclude the influence of different baseline signal levels and to show a more clear comparison between different working angles, we normalized the optical modulation strength to its maximum value. The normalized signal magnitude is used to represent the detection sensitivity.

Larger normalized signal magnitude indicates better detection sensitivity. Based on the results shown in figure 4, we can see that 89.3° with the biggest normalized signal magnitude is the optimal working angle between cross-polarizers for our optical setup. Meanwhile, these results also demonstrate the existence of a magic angle for our optical setup and agree with our theoretical calculation in section 2.4.1. When choosing the magic angle (89.3° for two-polarizer optical setup with CdTe crystal) as the working angle, we can have the highest detection sensitivity and smallest detection error. Compared to the detection sensitivity for 90°, the detection sensitivity at the magic angle is improved by around 10%.

3.2. Results of electric field distribution

3.2.1. Simulation results—Simulation results for different electric field distributions, including results of 3D electric field distribution, 2D electric field distribution and direction of scaled E at grid points, are shown in figures 5–7. Arrow direction is always from positive electric field to negative electric field. We can see that, within any detector crystals, the region closer to an electrode has a more dramatic change in electric field distribution than the region far from the electrode. We will discuss this point in section 4.

3.2.2. Pockels cell curve for different crystals—Pockels cell response curves obtained from CdTe crystals with different electrode patterns are shown in figure 8. We can see that the magnitude of Pockels cell response curve is smallest for 5×5 mm^2 square electrode (in CdTe), and largest for 2.5×2.5 mm^2 square electrode (in CdTe). The bias voltage remained at the same value throughout the whole measurement. We will discuss Pockels cell response curves in detail in section 4.

3.2.3. Experiment results of Ge-68 induced modulation signal—Figure 9 illustrates the modulation signal for CdTe. The definition of optical radiation strength is discussed in section 3.1. By analysing all '(MAX − MIN)/(MAX + MIN)' results, we could find the dependence of detection sensitivity on electrode distribution.

As shown in figure 10, the change of normalized optical modulation signal is a function of bias voltage when using CdTe as detector crystals. The optical modulation strength magnitude has been normalized to its maximum value. We can conclude that the change in optical modulation strength magnitude for CdTe crystal is largest for Pockels cell with 2.5×2.5 mm^2 square electrode and smallest for 5×5 mm^2 square electrode, which is discussed in section 4.

For all crystals, an increased crystal bias voltage leads to a stronger optical modulation strength for Ge-68 induced modulation signal. The modulation signal induced in CdTe tends to be saturated at bias voltages larger than 1300 V. We will discuss this point in section 4.

4. Discussion

4.1. Magic angle of setup

Figure 4 shows the dependence of the working angle between two crossed polarizers on detection sensitivity (presented by normalized signal magnitude). Our experimental results show that the magic angle of our optical setup with a CdTe detector crystal is around 89.3° based on figure 4. However, the magic angle varies for different experimental setups and even for the same experimental setup with different detector crystals and electrode geometry. Multiple factors, such as the extinction ratio of the polarizer (Kirkpatrick *et al* 1993), the light absorbing coefficient of the detector crystal (Seifert *et al* 2020), the surface condition of the crystal (Levchenko and Rappe 2008), electrode geometry (Karabey *et al* 2012) etc would greatly affect the value of the magic angle. Therefore, finding the magic angle for each optical setup is a prerequisite before using the optical setup to do other tests, in order to find the most sensitive operating point and reduce detection error.

In addition, we should note that we used the laser diode as the ionization source for measuring the magic angle of our setup. Compared with 511 keV photon irradiation, the laser diode has much higher photon flux and can be synchronous. Ionization from the laser diode is produced within the first few microns of the surface with which it interacts whereas the 511 keV ionization charge is deposited throughout the whole crystal. A laser diode could be used for finding the magic angle since there is no timing or energy requirement.

4.2. Matlab simulation results

From the comparison between 3D electric field distribution and 2D electric field distribution shown in figures 5–7, we can see that the electric field distribution experiences significant change with electrode geometry. Since electric field distribution will directly determine the signal modulation strength by the Pockels effect, different electrode geometries will impact our detected modulation signal and further affect our detection sensitivity. Looking at the simulation results of each electrode pattern, we could conclude that within any detector crystals, the region closer to an electrode has a more dramatic change in electric field distribution than the region far from the electrode. From results of both 2D electric field distribution and direction of scaled E at grid points, we can summarize that the central part of the detector crystal experiences nearly no change in electric distribution and thus the Pockels effect has little influence on this area. Therefore, to achieve a better detection sensitivity, we should place our pump laser close to an electrode for a larger divergence in electric field.

4.3. Pockels cell response curves of CdTe

We can see from figure 8 that multiple electrode dimensions have been investigated with CdTe detector crystal, which shows a larger response to the same stimulus as electrode dimension decreases. Small electrodes (such as square 2.5 × 2.5 mm^2) present the most obvious Pockels cell response among the three sizes of electrode. This phenomenon is mainly because electrode dimension will directly influence electric field distribution and thus influence the Pockels effect strength. For each electrode, the internal electric field is not constant and is the strongest in the vicinity of the electrode. Based on our simulation results,

there is a more dramatic internal electric field change for smaller electrode geometry and thus a more obvious Pockels effect modulation on optical signal. As a result, the polarization change is larger for the probe laser beam passing through a detector crystal with smaller electrodes, thereby leading to larger changes in signal detected by the photodiode. Consequently, choosing a smaller electrode (more concentrated electric field distribution) can improve the detection sensitivity.

4.4. Optical modulation signal with Ge-68

As discussed in section 2.5.4, we choose to read the stable signal level of each data point at five minutes after the ionization source was placed or removed. Due to the sensitivity limitation of our experimental setup, the signal will not change instantaneously during the transition between placing the source close to the detector crystal and moving the source away from the detector crystal. Depending on the source activity, the response to the presence or removal of the source may take a few seconds to a few minutes. After that, the signal level will remain stable around a fixed value. Therefore, we choose to wait five minutes for the signal to stabilize and then read each data point as the stable signal level.

However, this does not mean that the proposed experimental setup is limited to five minutes frame time. The signal level begins to change once the ionizing radiation source is placed near the detector crystal. This is an ultrafast process (under 10 ps). Therefore, searching for a faster readout method would be a subject for our future study. Our ultimate goal would be to establish a sufficiently sensitive setup (including the development of a suitable readout method) to measure the modulation signal from the ionizing charges created by one individual 511 keV photon with measured response time and variance both on the order of a picosecond. Once the single photon detection is achieved, we can monitor the modulation signal more rapidly and there will be no need to wait for 5 min to obtain a stable signal.

4.5. Experimental results of different electrode patterns with Ge-68 as the ionizing radiation source

From figure 10, we can see that the CdTe crystal with 2.5×2.5 mm^2 square electrodes leads to approximately double the modulation strength when compared to the CdTe crystal with 4×4 mm^2 square electrodes, and approximately four times the modulation strength compared to the CdTe crystal with 5×5 mm^2 square electrodes. Figure 10 also shows the dependence of modulation signal magnitude on crystal bias voltage for CdTe crystals, from which we can conclude that the modulation signal magnitude increases linearly with bias voltage before saturation. Higher bias voltages across the CdTe crystal can enhance the strength of optical modulation. The modulation signal induced in CdTe crystal is more likely to be saturated at bias voltages greater than 1300 V and further increasing the bias voltage may only contribute a small increment to the amplitude of modulation signal. Therefore, 1600 V is chosen as the optimal operating voltage for our future experiments.

In this paper, different detection sensitivity of three CdTe crystals is mainly caused by different dimensions of electrode pattern. During the process, the interaction between the Pockels cell and ionizing radiation photons would create a free ionization charge cloud. The application of a bias voltage across the crystal produces an internal weak current which can

force free charge carriers to move to their respective electrodes (electrons move to anode and holes move to cathode). By doing this, a smaller inner electric field opposite to the external electric field is created. The resistivity of the crystal is directly related to the internal current within the crystal which would affect the movement of free charge to electrode, and thus affect the detection sensitivity. Consequently, by analysing the results, our conclusion is:

- For any detector crystal, we could improve the detection sensitivity by improving the crystal's bias voltage to its saturation voltage and by using a smaller or more concentrated electrode to add bias voltage for crystal.

4.6. Potential detection structure with proposed detection setup for future practical PET module

Although in this paper we only investigated two immediate solutions to improve the detection sensitivity of the optical properties modulation based method for ionizing radiation detection, our ultimate goal is further improving the detection sensitivity of our setup and developing a detector module that is sensitive enough for measuring the signal induced by single 511 KeV photon interactions. After we could achieve this goal, we will start to design a practical detector structure using the basic cross-polarizers setup shown in figure 1. The practical structure will determined by the final well-developed experimental detection setup, but it should consist of a thicker detector crystal for improving the interaction probability between the photons and detector material. A compact geometry is another requirement, in order to increase the packing fraction during the detector module assembly. A schematic of a potential practical detector module is proposed in figure 11.

In the proposed structure of the detector module, a detector crystal with Pockels effect will be used to monitor the induced signal by the 511 keV photon interactions. The input probe laser and the reflected output laser light will be collimated and collected by a lens collimator. The input probe laser beam is composed of an ensemble of sub-laser beams with 200 μm diameter, consistent with Tao *et al* (2020) which demonstrated a 200 diameter laser beam could improve the detection sensitivity of optical properties modulation method. The polarization changes, the intensity or the phase of the reflected output laser will be modulated as long as the photons interact with the detector materials. The output laser will be detected directly by the photodetector.

5. Conclusions

In this work, we propose two methods to improve the detection sensitivity of an optical property modulation based ionizing radiation detection method for PET, using the two crossed polarizers setup. We first studied the magic angle of our setup and the results indicate the detection sensitivity of our setup could be improved by 10% at the magic angle (89.3° is the magic angle of our setup with CdTe crystal). But, the specific value of the magic angle should be calibrated for different experimental conditions. We also explored the relationship between detection sensitivity and electric field distribution in the detector crystal. A detector crystal with a smaller or more concentrated electrode geometry can provide better detection sensitivity. The detection sensitivity increases linearly with the crystal bias voltage, which means that a higher bias voltage could enhance the detection

sensitivity (up to the saturation point). Further increasing the bias voltage for CdTe could potentially further enhance the modulation strength and thus its detection sensitivity.

Acknowledgments

We acknowledge support from the National Institutes of Health under Award Number 5R01EB02390302 and R01EB028091. The authors would also like to thank Prof Jianfeng Xu and Prof. Qiyu Peng for the kindness discussion.

References

Bergeron M, Pepin CM, Cadorette J, Loignon-Houle F, Fontaine R and Lecomte R 2015 IEEE Trans. Nucl. Sci 62 36–41

Cates JW and Levin CS 2016 Phys. Med. Biol 61 2255–65 [PubMed: 26914187]

Cates JW and Levin CS 2018 Phys. Med. Biol 63 115011 [PubMed: 29762136]

Cates JW and Levin CS 2019 Phys. Med. Biol 64 175016 [PubMed: 31300623]

Chenault DB, Chipman RA and Lu SY 1994 Appl. Opt 33 7382–9 [PubMed: 20941299]

Collett E 2005 Field Guide to Polarization (Bellingham, WA: SPIE Press)

Daube-Witherspoon ME, Surti S, Perkins AE and Karp JS 2014 J. Nucl. Med 55 602–7 [PubMed: 24604909]

Dothager RS, Goiffon RJ, Jackson E, Harpstrite S and Piwnica-Worms D 2010 PLoS One 5 e13300 [PubMed: 20949021]

Fakhir GE, Surti S, Sheuermann J and Karp JS 2011 J. Nucl. Med 52 347–53 [PubMed: 21321265]

Gundacker S, Auffray E, Pauwels K and Lecoq P 2016 Phys. Med. Biol 61 2802–37 [PubMed: 26982798]

Gundacker S, Knapitsch A, Auffray E, Jarron P, Meyer T and Lecoq P 2014 Nucl. Instrum. Methods Phys. Res. A 737 92–100

Hecht S 1924 J. Gen. Physiol 7 235–67 [PubMed: 19872133]

Howe-Siang T, Ivan RP and Fayer MD 2005 J. Opt. Soc. Am. B 22 2009–17

Ironside C 2017 Linear Electro-Optic Effect, Electroabsorption and Electrorefraction (Bristol: IOP Publishing)

Karabey OH, Bildik S, Bausch S, Strunck S, Gaebler A and Jakoby R 2012 IEEE Trans. Antennas Propag 61 70–6

Kirkpatrick R et al. 1993 J. Chem. Soc., Faraday Trans 89 3297–9

Lecoq P 2012 IEEE Trans. Nucl. Sci 59 2313–8

Lecoq P 2017 IEEE Trans. Radiat. Plasma Med. Sci 1 473–85

Levchenko SV and Rappe AM 2008 Phys. Rev. Lett 100 256101 [PubMed: 18643676]

Li T, Esmaeelpour M and Levin CS 2018 Study of free carrier effects for an optical property modulation-based detector concept for PET 2018 IEEE Nuclear Science Symp. and Medical Imaging Conf. Proc. (NSS/MIC) pp 1–3

Loignon-Houle F, Pepin CM and Lecomte R 2014 Scintillation characteristics of 90% Lu LGSO with different decay times 2014 IEEE Nuclear Science Symp. and Medical Imaging Conf. (NSS/MIC) pp 1–3

Nemallapudi MV, Gundacker S, Lecoq P, Auffray E, Ferri A, Gola A and Piemonte C 2015 Phys. Med. Biol 60 4635–49 [PubMed: 26020610]

Pepin CM, Bergeron M, Thibaudeau C, Bureau-Oxton C, Shimizu S, Fontaine R and Lecomte R 2010 IEEE Trans. Nucl. Sci 57 1435–40

Seifert P, Lu X, Stepanov P, Durán Retamal JR, Moore JN, Fong KC, Principi A and Efetov DK 2020 Nano Lett. 20 3459–64 [PubMed: 32315186]

Surti S, Scheuerman J, EI Fakhri G, Daube-Witherspoon ME, Lim R, Abi-Hatem N, Moussallem E, Benard F, Mankoff D and Karp JS 2011 J. Nucl. Med 52 347–53 [PubMed: 21321265]

Tao L, Daghigian HM and Levin CS 2016 Phys. Med. Biol 61 7600–22 [PubMed: 27716640]

Tao L, Daghigian HM and Levin CS 2017 J. Med. Imaging 4 011010–011010

Tao L, Jeong D, Wang J, Adams Z, Bryan P and Levin CS 2020 Phys. Med. Biol 65 215021 [PubMed: 32707569]

Terance T 1969 Biopolymers 8 609–32

Tkachenko NV 2006 Optical Spectroscopy Methods and Instrumentations (Amsterdam: Elsevier)

Tokmakoff A 1996 J. Chem. Phys 105 1–12

Turkington TG and Wilson JM 2009 Attenuation artifacts and time-of-flight PET 2009 IEEE Conf. on Nuclear Science Symp p 2997–9

Turtos RM, Gundacker S, Lucchini MT, Procházková L, Čuba V, Burešová H, Mrázek J, Nikl M, Lecoq P and Auffray E 2016 Phys. Status Solidi RRL 10 843–7

Wang Y, Li Y, Li J, Xie S, Peng Q and Xu J 2019a Phys. Med. Biol 64 135017 [PubMed: 31117057]

Wang Y, Li Z and Xu J 2019b Investigation of Pockels effect in optical property modulation-based radiation detection method for positron emission tomography Medical Imaging 2019: Biomedical Applications in Molecular, Structural, and Functional Imaging vol 109531095306

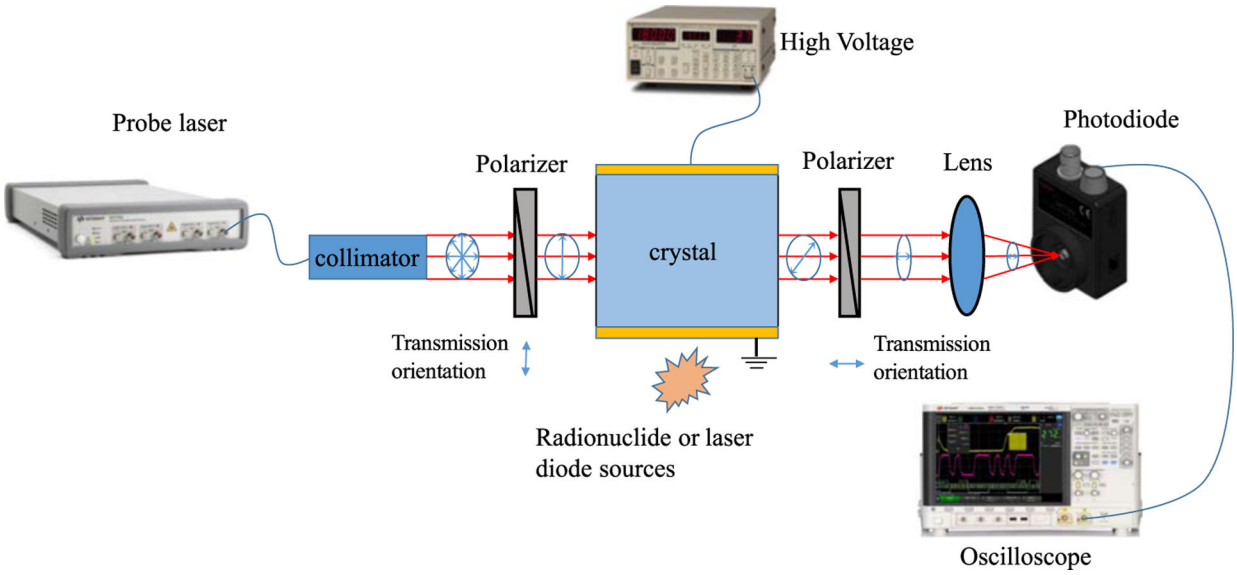

Figure 1.

Schematic diagram of optical setup based on two crossed polarizers. In the absence of an ionization source, the transmitted intensity is nominally zero.

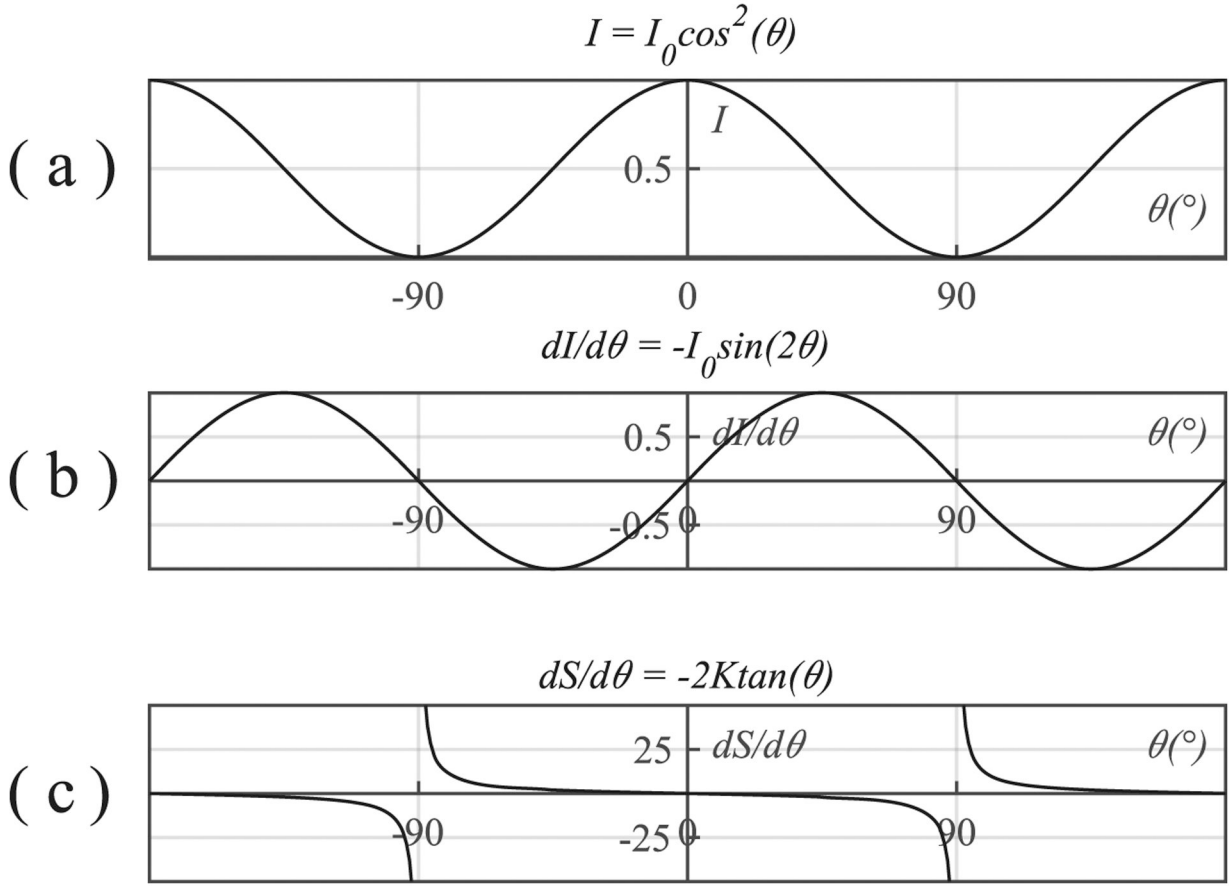

Figure 2.

(a) The dependence of light intensity I on the working angle θ between cross-polarizers, (b) the dependence of $dI/d\theta$ on the working angle θ, (c) the dependence of $dS/d\theta$ on the working angle θ.

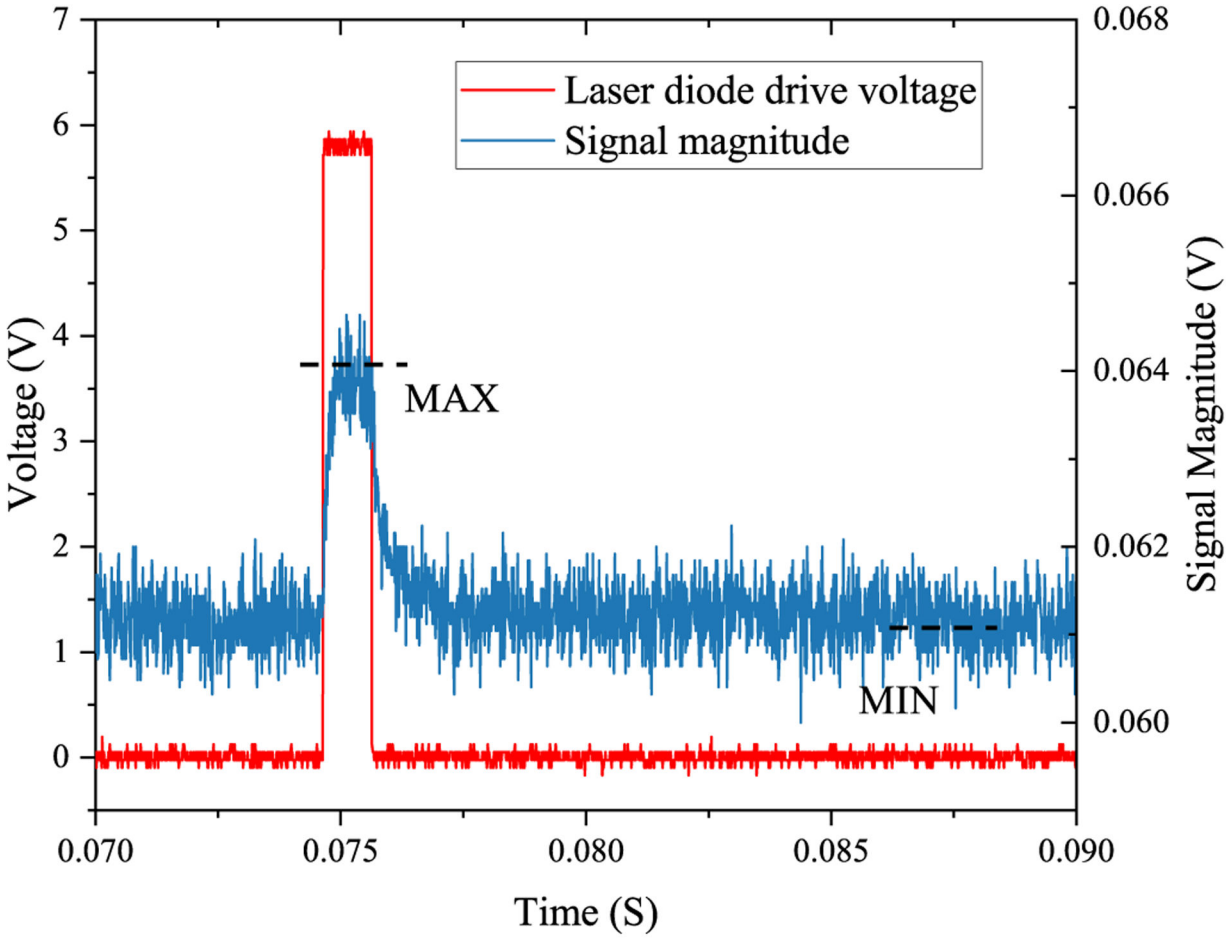

Figure 3.

Experimentally measured optical modulation signal induced by laser diode creating charge carriers at the surface of a CdTe crystal. The working angle is at 88.0°. Red line represents the drive voltage of laser diode, while the blue line indicates the changes in modulation signal level.

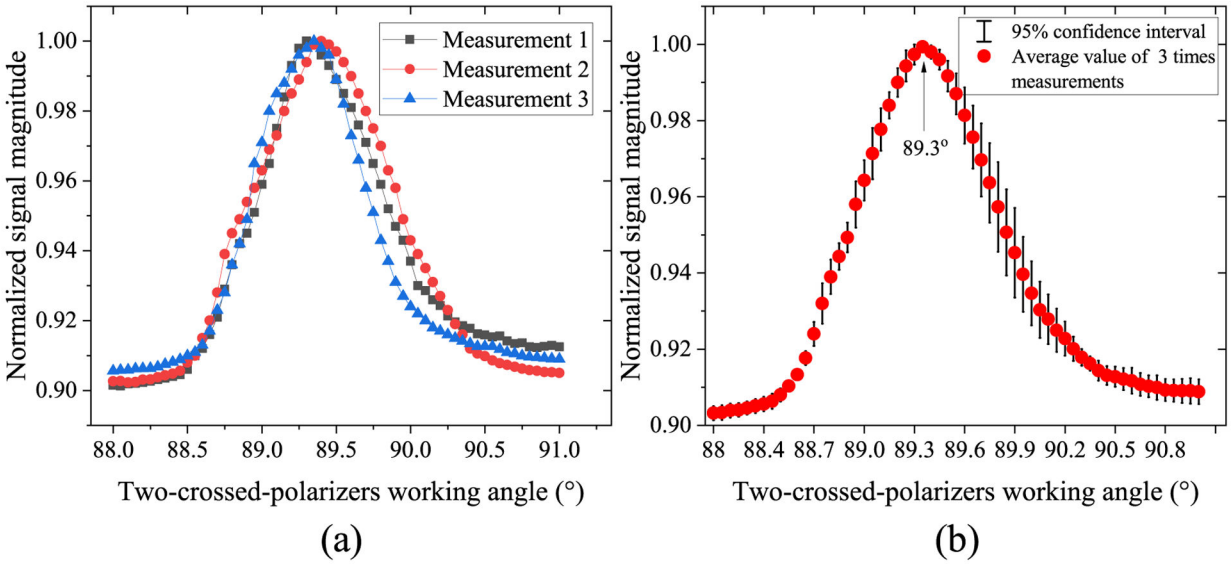

Figure 4.

Experiments results for the magic angle of CdTe crystal. (a) The relation between normalized signal magnitude and the two crossed polarizers working angle from three different experiments. (b) 95% confidence interval and average value of the three measurements. The relative detection sensitivity at the magic angle point is around 5%.

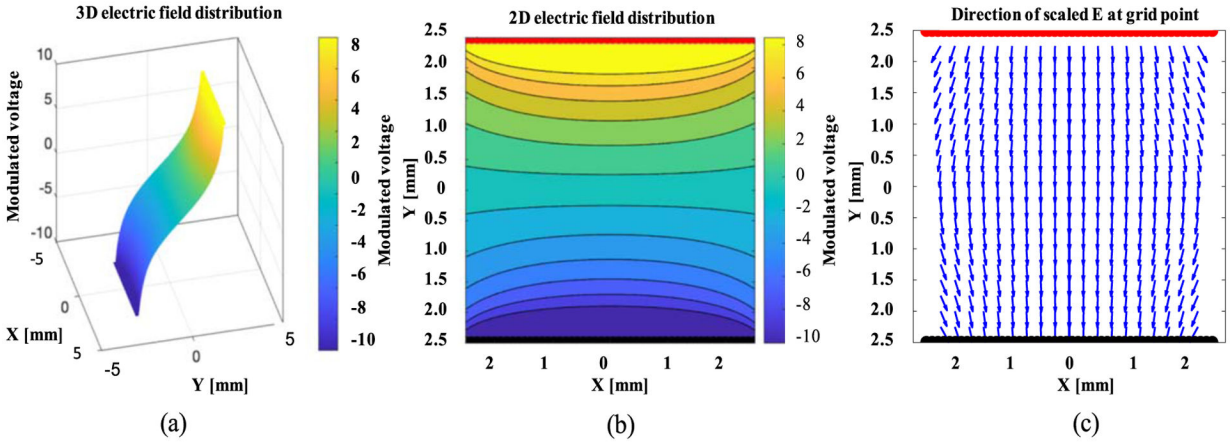

Figure 5.

Simulation results for CdTe crystal with 5.0 × 5.0 mm^2 square electrode, (a) 3D electric field distribution, (b) 2D electric field distribution and (c) direction of scaled E at grid points. Red line and black line represent the anode electrode and cathode electrode, respectively.

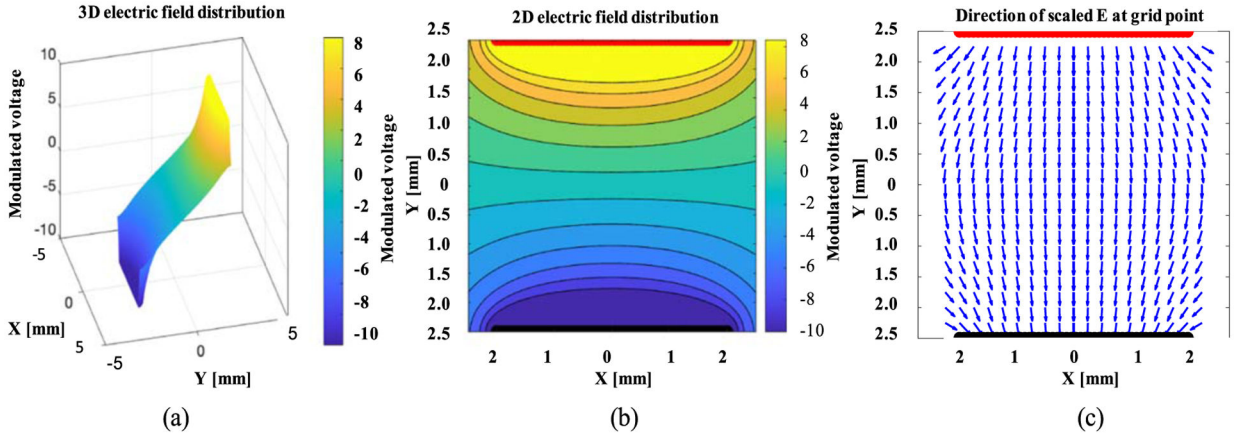

Figure 6.

Simulation results for CdTe crystal with 4.0 × 4.0 mm^2 square electrode, (a) 3D electric field distribution, (b) 2D electric field distribution and (c) direction of scaled E at grid points.

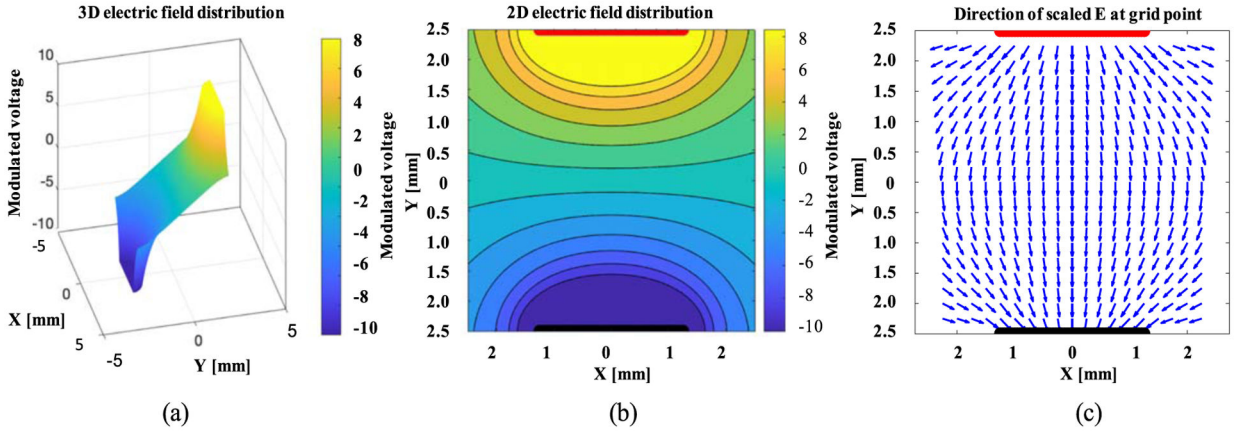

Figure 7.

Simulation results for CdTe crystal with 2.5 × 2.5 mm^2 square electrode, (a) 3D electric field distribution, (b) 2D electric field distribution and (c) direction of scaled E at grid points.

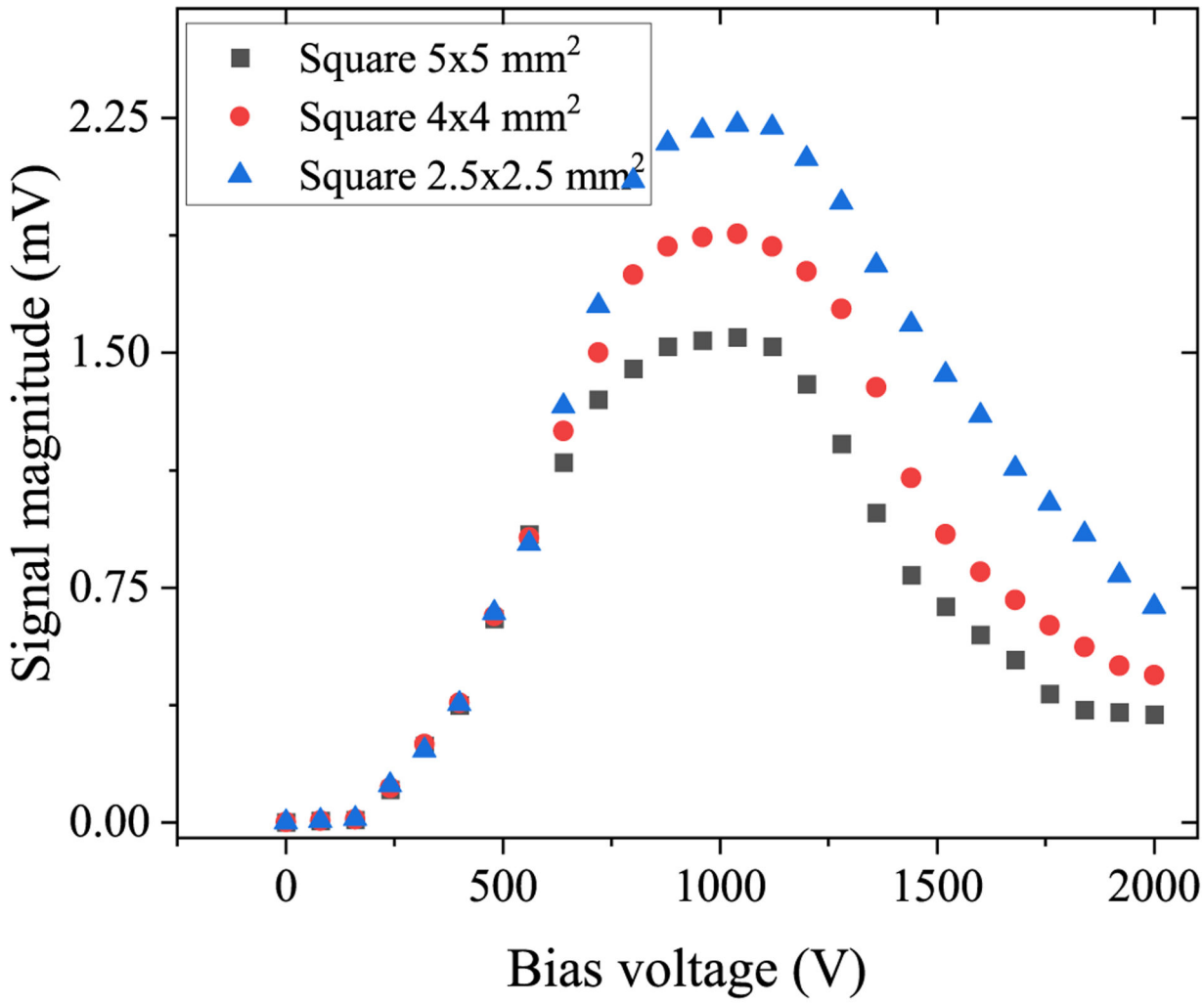

Figure 8.
Experimental results of Pockels cell response curve for CdTe with different square electrode patterns.

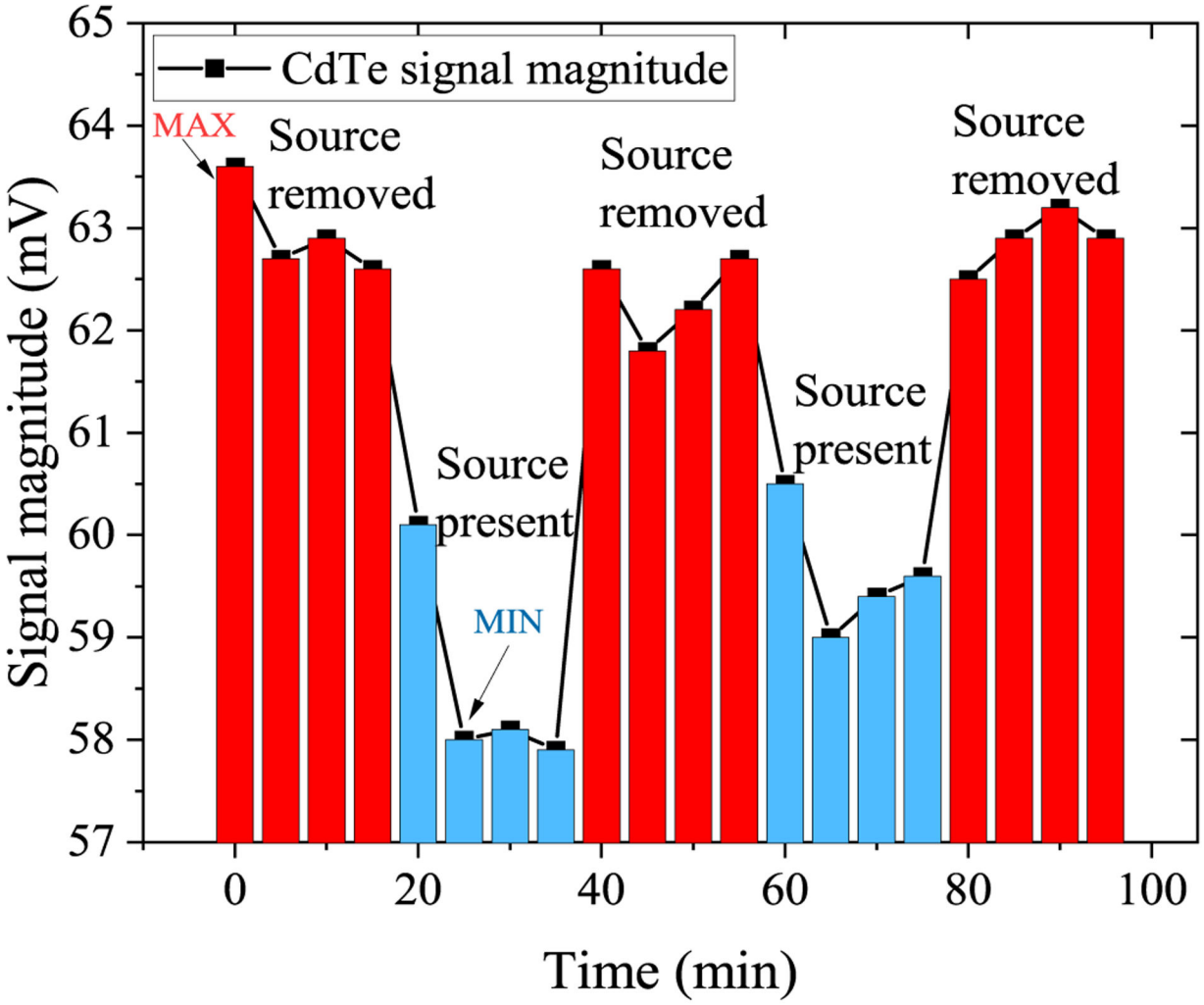

Figure 9.

The experimentally measured optical modulation signal results for CdTe with 1000 V bias voltage and induced by Ge-68. Blue bars indicates the magnitude of modulation signal when Ge-68 is placed 15 mm away from the crystal, whereas red bars represents the signal when the ionization source is removed.

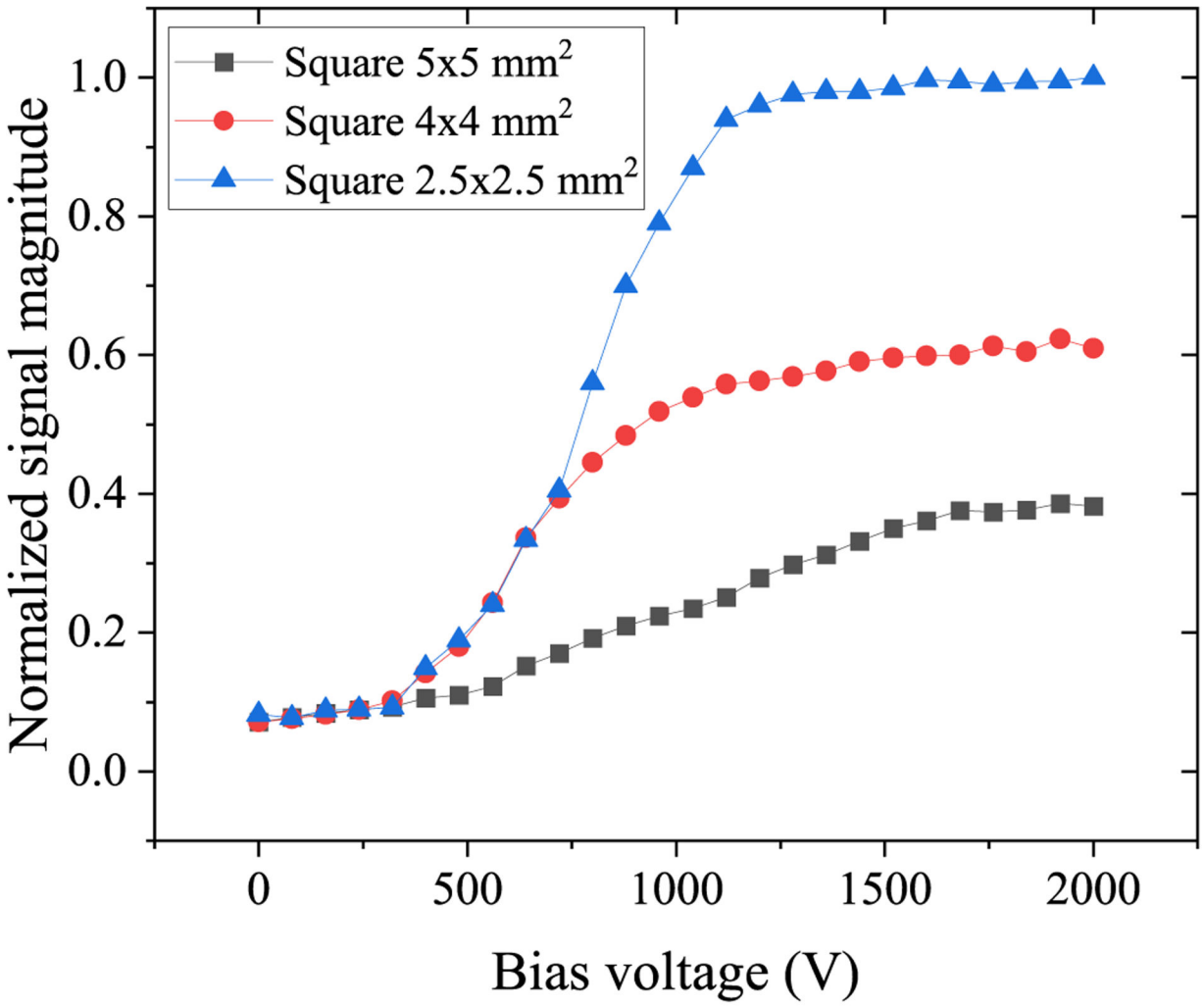

Figure 10.
The experimentally measured normalized modulation signal magnitude induced by Ge-68 source for CdTe with different electrode patterns.

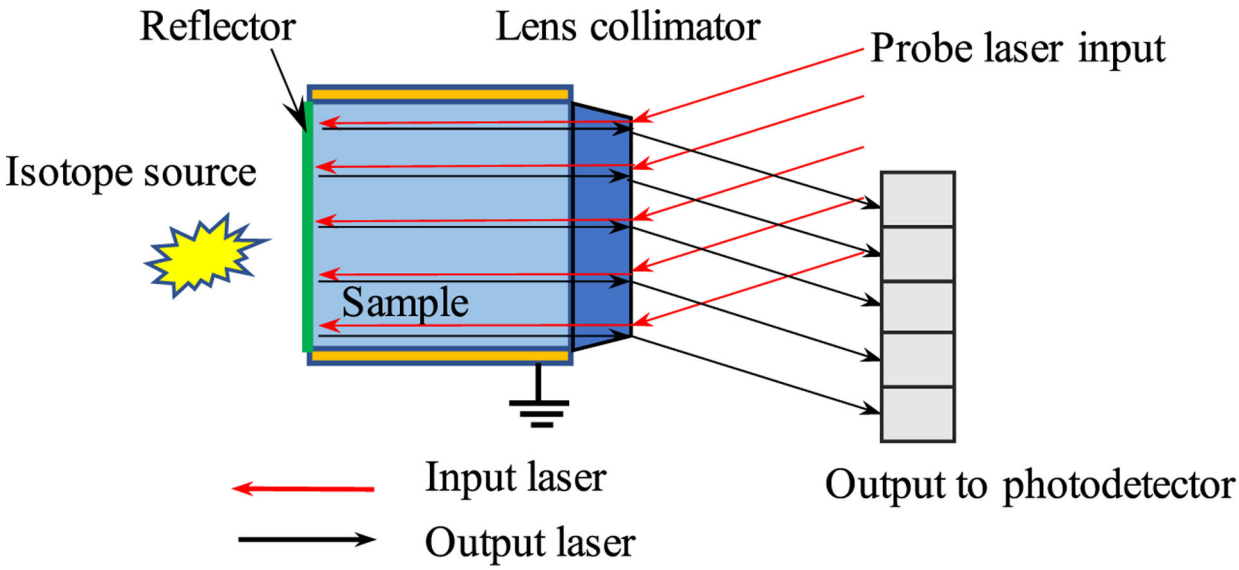

Figure 11.
Potential practical detector module using the proposed optical polarization modulation based detection mechanism. This module could be integrated together for assembling a practical PET system

Table 1.

The summary of the detector crystals' characteristics. The Pockels effect coefficient of CdTe was measured by Chenault *et al* (1994). The resistivity of CdTe was measured by Tao *et al* (2017).

Crystal	**CdTe**
Dimensions	$5 \times 5 \times 5$ mm^3
Purity	99.9%
Refractive index @ 1550nm	2.74
Density	5.85 g cm^{-3}
Effective Z number	50.2
Band gap energy	1.5 eV
Pockels effect coefficient	6.8 pm V^{-1}
Resistivity	19.6 MΩ · m

Table 2.

Summary for theoretical analysis of the magic angle of an optical setup based on two crossed polarizers.

θ°	Light intensity	Light intensity differential	Response differential	Detection error
0.0°	I_0(Max)	0	0	$2(I_o/K)$
45.0°	$I_o/2$	I_o (Max)	$2K$	$0.5(I_o/K)$
87.0°	$I_o/365$	0.1 I_o	$38K$	$0.002(I_o/K)$
90.0°	0	0	Infinity	0

I_O and K are two constant values in the table. Infinity means the value of detector response differential comes to infinity, which is based on equation (8).